Bio-Inspired Casein-Derived Antioxidant Peptides Exhibiting a Dual Direct/Indirect Mode of Action

Gizella Csire, François Dupire, Laetitia Canabady-Rochelle, Katalin Selmeczi, Loïc Stefan

Inorganic Chemistry

pubs.acs.org/IC Article

Bio-Inspired Casein-Derived Antioxidant Peptides Exhibiting a Dual Direct/Indirect Mode of Action

Gizella Csire, François Dupire, Laetitia Canabady-Rochelle, Katalin Selmeczi,* and Loic Stefan*

Cite This: https://doi.org/10.1021/acs.inorgchem.1c03085 Read Online

ACCESS | Metrics & More | Article Recommendations | Supporting Information

ABSTRACT: Antioxidant compounds are chemicals of primary importance, especially for their applications in nutrition and healthcare, thanks to their abilities to prevent oxidation processes and to limit and/or rebalance the oxidative stress, well-known for its impact on a wide variety of diseases. While several biomolecules are well-known for their antioxidant properties (*e.g.*, ascorbic acid, carotenoids, phenolic derivatives), bio-sourced antioxidants have drawn considerable attention in the last decades, especially bioactive peptides, mainly obtained by the hydrolysis process. Antioxidant peptide sequences are mainly identified a posteriori, thanks to fastidious and time-consuming approaches and techniques, limiting the discovery of new efficient peptides. In this context and taking inspiration from nature, we report herein on a new series of three bio-inspired antioxidant peptides derived from the milk protein casein. These phosphopeptides, designed to chelate the redox-active iron(III) and forming highly soluble complexes up to pH 9, act both as *indirect* (*i.e.*, inhibition of the metal redox activity) and *direct* (*i.e.*, radical scavenging) antioxidants.

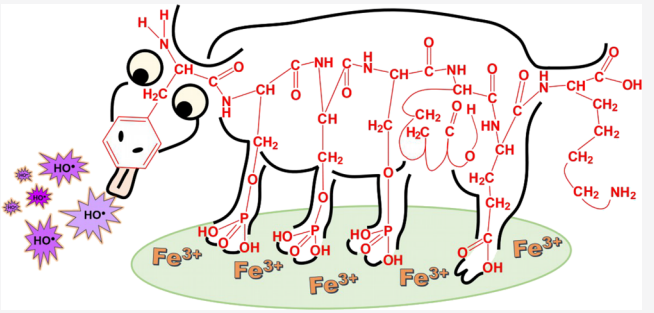

INTRODUCTION

Reactive oxygen species (or ROS) are essential highly reactive components for the proper functioning of the body, acting as signaling molecules to regulate biological and physiological processes.[1,2] In healthy organisms, the control of the ROS concentration is ensured by a complex endogenous antioxidant defense system involving enzymes, proteins, or other chemicals.[3] However, the presence of endogenous or exogeneous stresses can trigger a dysregulation of the ROS homeostasis, inducing the so-called oxidative stress reported to cause a wide variety of diseases.[4,5] In order to prevent oxidative stress and its detrimental effects, the intake of exogeneous antioxidants is an efficient strategy to rebalance the concentration of ROS. Depending on their inherent structure, antioxidants act according to two main modes of action: (i) *a direct mode of action* whereby the antioxidants directly react with the ROS;[3,6,7] (ii) *an indirect mode of action* whereby the antioxidants hinder the biometal-induced redox aerobic process *via* the chelation of specific transition metals. Indeed, *in vivo*, copper and iron are involved in the production of ROS through the catalytic reduction of molecular oxygen (O_2) to the superoxide anion radical ($O_2^{\cdot-}$), and subsequently to hydrogen peroxide (H_2O_2) and a hydroxyl radical ($HO^{\cdot}$) (Figure 1a). Thus, their chelation induces a decrease of the ROS production and positive effects on ROS-mediated pathologies.[3,8−10] Numerous metal-chelating antioxidants have been reported[3,8−11] and, recently, peptides have emerged as new bio-sourced antioxidants.[12−14] Peptides have been already considered as therapeutics offering high selectivity and effectiveness, safety, and tolerability,[15,16] and biologically relevant peptides can be synthesized using proven, fast, and efficient methods.[17] Up until now, the majority of antioxidant peptides have been identified through tandem LC/MS/MS analyses from protein hydrolysates of natural resources[12−14,18,19] known for their antioxidant properties. However, this serendipitous approach is hazardous, fastidious, and time-consuming, severely limiting the discovery of new effective antioxidant peptides. Thus, we believe that a more rational approach based on a finely tailored bio-inspired molecular design could achieve the same goal in a more judicious and efficient way. While a large body of work concerning copper-chelating peptides has been reported in the recent years,[20,21] the development and studies of iron-chelating peptides are still in their infancy and remain challenging. However, iron is present in the body in iron labile pools in which iron is not or slightly chelated and therefore accessible to exogeneous antioxidants,[22,23] including in the lysosomes where iron is in its free Fe(III) form.[22,24] For these reasons and because Fe(III) is in a biologically unusual +III oxidation state, we focus our attention on the development of antioxidant Fe(III)-

Received: October 4, 2021

https://doi.org/10.1021/acs.inorgchem.1c03085
Inorg. Chem. XXXX, XXX, XXX−XXX

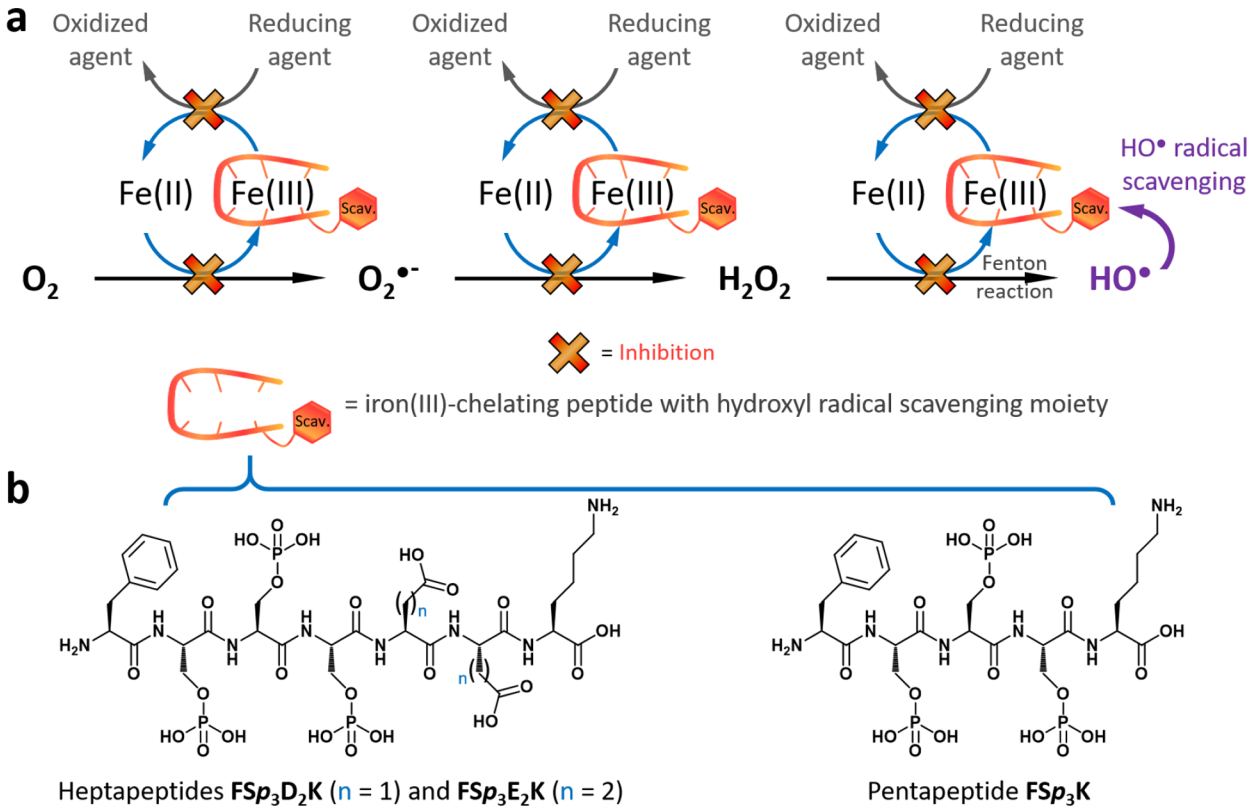

Figure 1. (a) Schematic representation of the *indirect* (*i.e.*, inhibition of the metal redox activity) and *direct* (*i.e.*, radical scavenging) antioxidants mode of actions and (b) chemical structures of the three phosphopeptides studied.

chelating peptides with both indirect and direct modes of action (Figure 1a). While a first series of efficient antioxidant pentapeptide has been previously reported by our group,[25] we would like to report herein on new bioinspired phosphopeptides offering both high antioxidant properties and high Fe(III)-chelating capabilities.

RESULTS AND DISCUSSION

Bioinspired Design and Synthesis of Antioxidant Phosphopeptides. To design such compounds, we took inspiration from dietary phosphoproteins well-known for their iron-chelating abilities, such as the egg yolk phosvitin[26] or the milk caseins.[27] In particular, caseins are a family of four proteins termed α_{S1}-, α_{S2}-, β-, and κ-caseins in which phosphorylation occurs at the serine residues and reported for their antioxidant properties.[28,29] Interestingly, a specific recurring sequence of five amino acids, termed cluster, comprising three phosphoserines (noted S*p*) followed by two glutamic acids (E), *i.e.*, an S*p*S*p*S*p*EE cluster, appears once in the β-casein and α_{S1}-casein, and twice in the α_{S2}-casein.[30−32] Based on these observations and on our previous work,[25] we design a first heptapeptide FSp_3E$_2$K (Figure 1b) comprised of the above-mentioned casein-derived cluster on which we grafted (i) a lysine (K) at the C-term bringing an additional charge to improve the peptide solubility at neutral pH, and (ii) a phenylalanine (F) at the N-term to provide a further antioxidant property to the peptide, *i.e.*, a direct mode of action based on the ability of phenylalanine to entrap hydroxyl radicals (*vide infra*). To evaluate the impact of the two acidic side chains on the chelation and antioxidant properties, two other compounds have been considered: the heptapeptide FSp_3D$_2$K in which the glutamic acids have been replaced by aspartic acids, and the acidic side chain-lacking pentapeptide FSp_3K in which the two E have been removed. The three phosphopeptides were synthesized, purified, and fully characterized (Supporting Information (SI), part 2).

Evaluation of the Direct and Indirect Antioxidant Properties. To evaluate the antioxidant performance of the three Fe(III)-chelating peptides, we carried out a series of three complementary assays, namely, ascorbate,[33] Amplex Red,[34] and 3-CCA (for coumarin-3-carboxylic acid)[35] tests to measure the iron redox activity (*i.e.*, the reducibility of Fe(III) to Fe(II)) and the formation of H_2O_2 and HO$^{\bullet}$, respectively. To assess the antioxidant power of the three Fe(III)-chelating phosphopeptides, two compounds were selected as references: the positive control is the deferoxamine (DFO), an approved siderophore drug used to treat iron overload and exhibiting antioxidant properties both *in vitro*[36−38] and *in vivo*,[39] whereas the negative control is the ethylenediaminetetraacetic acid (EDTA), well-known for its good chelation abilities but weak antioxidant properties.[36,37,40]

Thus, employing the ascorbate test, a first series of experiments were carried out with 1 equiv Fe(III) for 1 equiv ligand at physiological pH 7.4. As depicted in Figure 2a, the maximum AscH$^-$ consumption is observed for EDTA (negative control) with 64.2 μM consumed after 10 min. Interestingly, when phosphopeptides were used, this value drastically drops to 15.0 μM for the casein cluster-derived heptapeptide FSp_3E$_2$K, to 12.7 μM for the other heptapeptide FSp_3D$_2$K, and to 11.0 μM for the shortest FSp_3K. These data highlight the efficiency of the three peptides to reduce the redox process of the metal ion from 77% (FSp_3E$_2$K) to 83% (FSp_3K) compared to EDTA, even if the positive control DFO appears slightly more efficient (−96%, 2.5 μM AscH$^-$

https://doi.org/10.1021/acs.inorgchem.1c03085
Inorg. Chem. XXXX, XXX, XXX−XXX

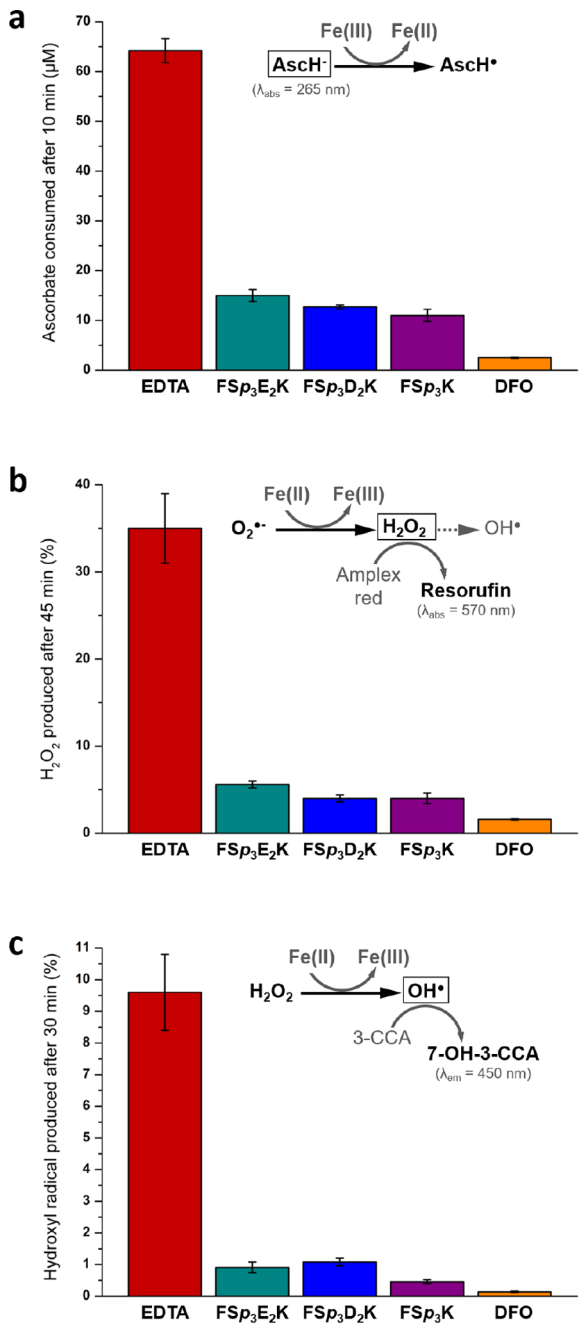

Figure 2. Evaluation of the antioxidant properties of all the phosphopeptides and of the negative (EDTA) and the positive (DFO) reference compounds. The corresponding reactions involved for each assay are inserted in each graph, with their corresponding absorbance or emission wavelengths. All experiments were carried out at pH 7.4 with (a) $[AscH^-] = [Ligand] = [Fe(III)] = 100\ \mu M$, in 50 mM HEPES, (b) $[AscH^-] = 200\ \mu M$, $[Ligand] = [Fe(III)] = 50\ \mu M$ (except $[EDTA] = [Fe(III)] = 10\ \mu M$), in 50 mM HEPES, and (c) $[AscH^-] = 125\ \mu M$, $[Ligand] = [Fe(III)] = 50\ \mu M$ (except $[EDTA] = [Fe(III)] = 5.0\ \mu M$ and $[AscH^-] = 12.5\ \mu M$) in water.

consumed, Table S1). To gain further insights into the antioxidant properties of the three phosphopeptides, we then measured their abilities to limit the formation of two distinct ROS, namely, H_2O_2 and HO$^{\cdot}$. Considering the negative control EDTA in the presence of 1 equiv Fe(III), the amount of H_2O_2 formed after 45 min is equal to 35.0% relative to the concentration of the complex (Figure 2b, Table S2). By contrast, this value drops to 1.6% when the positive control DFO is used. Phosphopeptides also exhibit significant antioxidant properties, with an amount of H_2O_2 produced from 5.6% for FSp_3E$_2$K to 4.0% for both FSp_3D$_2$K and FSp_3K. Interestingly, the glutamic acid-incorporating peptide FSp_3E$_2$K with the closest casein cluster-like sequence has the weaker antioxidant efficiency compared to the two others, as previously observed in the $AscH^-$ test (Figure 2a). Subsequently, 3-CCA experiments were carried out, and results (Figure 2c) highlight once more that the highest quantity of HO$^{\cdot}$ (9.6%, corresponding to the formed HO$^{\cdot}$/Fe(III)-complex ratio) is formed in the presence of EDTA. Oppositely, DFO and phosphopeptides show better antioxidant activities, with a ratio of HO$^{\cdot}$ produced of 0.14% for DFO, while this value spans from 1.08 (for FSp_3D$_2$K) to 0.46% (FSp_3K) for our compounds (Table S3). These experiments confirm that all the three phosphopeptides act as effective antioxidants, slightly less efficient than DFO but highly better than EDTA.

However, these peptides have also been designed to behave as direct antioxidants through the entrapment of the most reactive ROS, *i.e.*, the hydroxyl radical HO$^{\cdot}$. Indeed, the oxidation of phenylalanine to tyrosine by HO$^{\cdot}$ has already been reported as a marker of oxidative stress.[41,42] To follow the oxidation of the Phe moiety, a first series of four experiments per peptide was performed by HRMS/MS.[25] Thus, the MS spectrum (direct injection) of a stoichiometric peptide/Fe(III)/$AscH^-$/H_2O_2 solution for the heptapeptide FSp_3D$_2$K (Figure S8, SI for FSp_3E$_2$K (Figure S14), and FSp_3K (Figure S2)) shows the presence of the native heptapeptide (m/z = 513.124 $[M + 2H]^{2+}$), the FSp_3D$_2$K-iron(III) complex (m/z = 539.579 $[M\text{-}H + Fe]^{2+}$), which confirms the Fe(III)-chelating properties of the peptide (discussed hereinafter), and of another peak at m/z = 521.123 corresponding to the mono-oxidized peptide $[M + 2H + O]^{2+}$. To separate and precisely analyze each of these species, all the samples were injected in RP-HPLC/HRMS/MS, and the chromatogram for FSp_3D$_2$K (Figure 3a, SI part 4 for FSp_3E$_2$K and FSp_3K) reveals the presence of the native peptide (retention time t_R = 13.4 min), preceded by a set of three peaks with shorter retention times (t_R = 10, 11, and 12.2 min). The latter ones correspond to the mono-oxidized $[M + 2H + O]^{2+}$ species attributable to the oxidation of the phenyl ring of the N-term phenylalanine to its monohydroxy-equivalent as determined by HRMS/MS fragmentation (Figure 3b). The use of HPLC allows us to separate the three phenolic isomers,[43,44] *i.e.*, the peptides containing the *ortho*-, *meta*-, and *para*-hydroxyphenylalanine, indicative of the reaction of the HO$^{\cdot}$ with all positions of the phenyl ring. Interestingly, working with harsher conditions (*i.e.*, FSp_3D$_2$K/Fe(III)/$AscH^-$/H_2O_2 1/1/10/10) in order to shift the reaction equilibrium, we observed the formation of additional broad peaks (in green, Figure 3c) with shorter t_R = 7.5 to 8.9 min characterized by m/z = 529.116 corresponding to the di-hydroxylated peptide $[M + 2H + 2O]^{2+}$, *i.e.*, the peptide in which the phenylalanine has been oxidized twice (Figure 3d). These experiments confirm the ability of our phosphopeptides to selectively react with HO$^{\cdot}$ (control experiments were carried out to discard the possibility of a H_2O_2-induced oxidation, SI part 4) *via* the N-term phenylalanine, validating the relevance of our approach and the direct antioxidant mode of action of our designed peptides. Lastly, the HPLC/HRMS chromatograms also highlight the presence of the mononuclear peptide-Fe(III) complex (t_R =

https://doi.org/10.1021/acs.inorgchem.1c03085
Inorg. Chem. XXXX, XXX, XXX−XXX

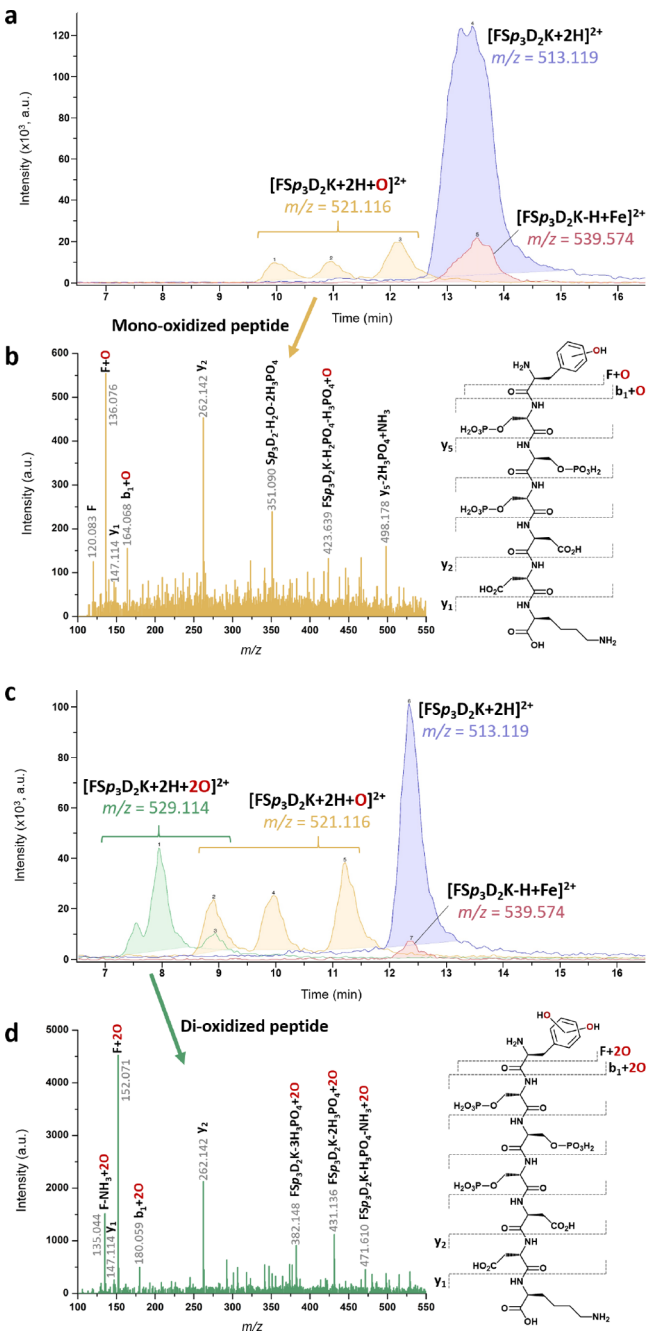

Figure 3. HPLC-HRMS chromatograms highlighting (a) the mono-oxidation of FSp_3D_2K ([Fe(III)] = [FSp_3D_2K] = [$AscH^-$] = [H_2O_2] = 1 mM), and (c) the di-oxidation of FSp_3D_2K ([Fe(III)] = [FSp_3D_2K] = 1 mM, [$AscH^-$] = [H_2O_2] = 10 mM). Corresponding HRMS/MS spectra of the (b) mono-oxidized peptide at m/z = 521.116 and (d) di-oxidized peptide at m/z = 529.114. Experiments were carried out at pH 7.4 in water.

13.5 min, m/z = 539.574 $[M-H+Fe]^{2+}$ for FSp_3D_2K (in red, Figure 3a); see SI part 4 for FSp_3E_2K and FSp_3K), which have been further characterized using potentiometric measurements, circular dichroism (CD), and ^{31}P NMR spectroscopies (SI part 5A,B).

Studies on the Phosphopeptides Chelation Properties. First, potentiometric studies were carried out on the synthesized compounds, in the presence and absence of Fe(III), to both access the species distributions as a function of pH and to obtain characteristic thermodynamic constants (protonation, complexation) of the peptides and iron(III) complexes. The deprotonation constants of each ligand alone (*i.e.*, in the absence of Fe(III)) are reported in Table 1.

Table 1. Overall Protonation Constants (logβ H_iL) and Deprotonation Constants (pK) of the Studied Peptides; T = 298 K, I = 0.1 M $NaNO_3$ (Standard Deviations Are in Parentheses)

logβ	FSp_3K	FSp_3E_2K	FSp_3D_2K
HL	10.90 (4)	11.36 (1)	11.43 (1)
H_2L	19.16 (6)	19.90 (2)	20.01 (2)
H_3L	26.31 (6)	27.28 (2)	27.43 (2)
H_4L	32.49 (7)	33.86 (2)	34.02 (2)
H_5L	38.18 (8)	39.66 (3)	39.82 (3)
H_6L	42.27 (12)	44.74 (3)	44.72 (3)
H_7L		49.12 (3)	48.85 (3)
H_8L		52.78 (5)	52.37 (5)
pK			
$COOH_{term}$	4.09 (12)	3.66 (5)	3.52 (5)
COOH (1)		4.38 (3)	4.13 (3)
COOH (2)		5.08 (3)	4.90 (3)
$PO_3(OH)^-$ (1)	5.69 (8)	5.80 (3)	5.80 (3)
$PO_3(OH)^-$ (2)	6.18 (7)	6.58 (2)	6.59 (2)
$PO_3(OH)^-$ (3)	7.15 (6)	7.38 (2)	7.42 (2)
NH_3^+ (N_{term})	8.26 (6)	8.54 (2)	8.58 (2)
εNH_3^+ (Lys)	10.90 (4)	11.36 (1)	11.43 (1)

Depending on the peptide sequence, these ligands have 9 (FSp_3K) or 11 (FSp_3D_2K, FSp_3E_2K) protonable groups, notably one or three carboxylate ($COOH/COO^-$), three phosphates ($PO_2(OH)_2/PO_4^{2-}$), and two amino ($-NH_3^+/-NH_2$) groups. The first pK of phosphate groups ($PO_2(OH)_2/PO_3(OH)^-$) is too low to be easily determined in titration experiments. Thus, the first measured dissociation step corresponds to the deprotonation of terminal COOH whose value is considerably higher ($pK_{COOHterm}$ = 3.52−4.09) than the pK value of free amino acids (2.0−2.5). This increase in the pK values is probably due to the large network of hydrogen bonds formed between the negatively charged phosphate groups (as H acceptors) and the protonated amine and COOH groups (as H donors). This H-bond network has also an impact on the deprotonation process of terminal NH_2 (pK_{Nterm} = 8.26−8.58) and lysine NH_2 (pK_{Lys} = 10.90−11.43) groups, whose pK values are therefore higher than those observed for the first series of pentapeptide FD_3K (pK_{Nterm} = 7.64, pK_{Lys} = 10.98) and FE_3K (pK_{Nterm} = 7.50, pK_{Lys} = 10.82).[25] In the case of FSp_3D_2K, FSp_3E_2K peptides, two additional deprotonation steps were measured corresponding to the dissociation of aspartic and glutamic acid side chains ($pK_{COOH(1)}$ = 4.13 and 4.38, $pK_{COOH(2)}$ = 4.90 and 5.08 for FSp_3D_2K and FSp_3E_2K, respectively). These pK values are similar to those measured for the previously studied peptides,[25] showing that these groups are not involved in inter- or intramolecular interactions. Regarding the $PO_3(OH)^-/PO_4^{2-}$ dissociation processes of three phosphate groups in the peptide sequence, the consecutive pK values are well separated ($\Delta pK \approx 0.6-0.9$) and the first $pK_{PO3(OH)-(1)}$ value (5.69−5.80) corresponds well to those of phosphoserine alone ($pK_{PO3(OH)-serine}$ = 5.61).

Then, stability constants (logβ) and stepwise deprotonation constants (pK) of iron(III) complexes were assessed and are

https://doi.org/10.1021/acs.inorgchem.1c03085
Inorg. Chem. XXXX, XXX, XXX−XXX

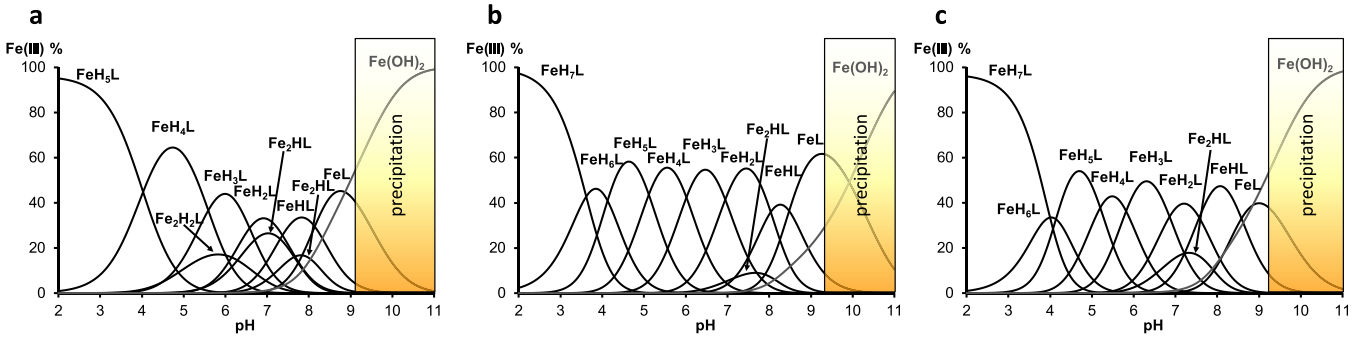

Figure 4. Speciation diagrams of Fe(III)-phosphopeptides 1:1 systems: (a) Fe(III)−FSp_3K, (b) Fe(III)−FSp_3D_2K and (c) Fe(III)−FSp_3E_2K. For all experiments, $[peptide]_{tot}$ = 2.0 mM, T = 298 K, and I = 0.1 M $NaNO_3$.

summarized in Table 2 and Figure 4. The results indicate that mono- and binuclear complexes were formed, while bis(ligand) complexes were not observed. For all the three phosphopeptides and at pH 2, the second deprotonation of one phosphate group occurs, meaning that the complexation of iron(III) is already performed by mono- and di-deprotonated phosphate groups. Accordingly, potentiometric titrations start with the species FeH_5L for FSp_3K and FeH_7L for both FSp_3D_2K and FSp_3E_2K. The following steps up to the formation of FeH_4L species correspond to the deprotonation of $COOH_{term}$ for the three phosphopeptides and also to the deprotonations of COOH(1) and COOH(2) in the case of FSp_3D_2K and FSp_3E_2K. The next two dissociation steps belong to the formation of the FeH_3L and FeH_2L complexes where the other two phosphate groups are deprotonated. All these pK values from pK(FeH_7L/FeH_6L) to pK(FeH_3L/FeH_2L) are close to the corresponding pK values in the ligands alone (Table 1), demonstrating that the metal ion-promoted dissociation process does not occur. The H-bond network, operating in the solution of phosphopeptide alone, cannot be formed with terminal NH_3^+ because the phosphate groups are coordinated to the metal ion; thus, the pK_{Nterm} (FeHL formation) value is decreased to 7.37−8.04, a value close to that observed with the previous FD_3K series.[25] The last dissociation step corresponds to water deprotonation coordinated to the metal ion with a pK value of 8.14, 8.48, and 8.58 for FSp_3K, FSp_3D_2K, and FSp_3E_2K, respectively. At a concentration of 100 μM and at pH 7.4, while small precipitation occurred in the presence of FD_3K, homogeneous solutions were detected with the phosphorylated FSp_3K, FSp_3D_2K, and FSp_3D_2K peptides. At this pH, the pFe value is, for instance, 1.5 logarithmic units higher for FSp_3D_2K (pFe = 14.3) than for FD_3K (pFe = 12.8),[25] highlighting that the presence of phosphoserines in the sequences significantly increases the stability of the formed iron(III) complexes and are able to prevent metal ion hydrolysis up to pH 9.2. Based on all these data (potentiometric and spectroscopic, SI part 5), it can be reasonably assumed that the mononuclear 1:1 Fe(III):peptide complexes are formed through the chelation of the metal ion mainly by the phosphate groups, even if other functions (*e.g.* carboxylate) and/or water can be involved in the chelation as previously reported.[25] However, to decipher the precise complex structures of these phosphopeptides, further investigations are required. Interestingly, such data both confirm and bring new insights into the role of the casein cluster Sp_3E_2 on the chelation and antioxidant properties of milk casein proteins, as already reported.[27−32]

Finally, since our phosphopeptides are derived from a specific sequence of casein, a milk protein well-known for its ability to bind calcium mainly through its phosphoserines,[45,46] we performed competition experiments in the presence of calcium ions. Using the $AscH^-$ test, no loss of antioxidant activity is observed upon addition of 1 and 10 equiv of the non-redox active Ca(II) to a 1:1 mixture of Fe:peptide (Table S1); conversely, a sensitive decrease of the ascorbate consumption, *i.e.*, a better antioxidant activity, appears. Additional CD, ^{31}P NMR, and ESI-MS studies of the Fe(III):Ca(II):phosphopeptide ternary systems (Figures S23−S27) show that iron remains chelated even with excess calcium and suggest a possible reorganization of the peptides around Fe(III) in the presence of Ca(II) (SI part 5B), confirming the efficiency and selectivity of our bioinspired antioxidant phosphopeptides.

Table 2. Stability Constants (logβ) and Derived Data (pK) for Fe(III) Complexes of the Studied Peptides; T = 298 K, I = 0.1 M $NaNO_3$ (Standard Deviations Are in Parentheses)

logβ	FSp_3K	FSp_3E_2K	FSp_3D_2K
FeH_7L		59.24 (5)	60.32 (4)
FeH_6L		55.24 (7)	56.70 (4)
FeH_5L	48.19 (6)	51.10 (5)	52.57 (4)
FeH_4L	44.16 (5)	45.90 (6)	47.45 (3)
FeH_3L	38.57 (6)	40.08 (5)	41.43 (3)
FeH_2L	31.99 (7)	33.22 (6)	34.48 (3)
FeHL	24.62 (6)	25.65 (3)	26.44 (2)
FeL	16.48(5)	17.07 (5)	17.96 (3)
Fe_2H_6L		62.05 (7)	62.83 (6)
Fe_2H_5L		58.78 (7)	59.99 (4)
Fe_2H_4L	50.71 (8)	54.81 (6)	56.20 (4)
Fe_2H_3L	47.70 (6)	49.87 (6)	51.54 (4)
Fe_2H_2L	43.07 (6)	44.33 (5)	45.86 (4)
Fe_2HL	36.78 (6)	37.73 (5)	39.09 (4)
Fe_2L	29.13 (10)		
pK (FeH_7L/FeH_6L)		4.00	3.62
pK (FeH_6L/FeH_5L)		4.14	4.13
pK (FeH_5L/FeH_4L)	4.03	5.20	5.12
pK (FeH_4L/FeH_3L)	5.59	5.82	6.02
pK (FeH_3L/FeH_2L)	6.58	6.86	6.95
pK (FeH_2L/FeHL)	7.37	7.57	8.04
pK (FeHL/FeL)	8.14	8.58	8.48

CONCLUSIONS

Thus, we reported herein on the rational design of an original series of bioinspired casein-derived phosphopeptides exhibiting

https://doi.org/10.1021/acs.inorgchem.1c03085
Inorg. Chem. XXXX, XXX, XXX−XXX

significant antioxidant properties thanks to a dual mode of action. Indeed, these compounds show high Fe(III)-chelating abilities with stability of the complexes formed up to pH 9.2, leading to indirect antioxidant activities. Concomitantly, the direct antioxidant behavior is provided by the phenylalanine moiety and its inherent abilities to act as radical scavenger, especially for the highly reactive hydroxyl radical, as observed by HRMS experiments. Altogether, these two combined antioxidant effects brought by the phosphopeptides reduce, *inter alia*, the metal redox process to 83% and the formation of $HO^{\cdot}$ to −95%.

Also, our study highlights that to design effective antioxidant peptides, the incorporation of aromatic amino acid(s) (herein, phenylalanine) is an easy way to induce a direct antioxidant mode of action (*i.e.*, radical scavenging), while the presence of highly chelating amino acids (herein, phosphoserines) are required to assess both an efficient Fe(III) chelation and effective indirect antioxidant properties.

MATERIAL AND METHODS

Peptide Synthesis (General Procedure). The three peptides were synthesized at a 200 μmol scale using an automated ResPep XL synthesizer (Intavis AG) using an Fmoc/tBu strategy and double couplings for each amino acid. Preloaded Wang-resin (0.70 mmol·g^{-1}, 200−400 mesh) was used. The standard conditions for each coupling were Fmoc-amino acid (5 equivalents), 2-(1*H*-benzotriazol-1-yl)-1,1,3,3-tetramethyl-uronium tetrafluoroborate (HBTU, 5 equivalents), and 4-methylmorpholine (NMM, 10 equivalents) in dimethylformamide (DMF) and *N*-methyl-2-pyrrolidone (NMP), with a coupling time of 60 min. Fmoc-Ser(PO(OBzl)OH)-OH was introduced at 4.0 equiv using HBTU (4.0 equiv), NMM (8.0 equiv) in DMF, and NMP. Fmoc-deprotection steps were carried out using a 20% piperidine solution in DMF (3 × 15 min), and final cleavages were achieved using a trifluoroacetic acid/triisopropylsilane/water (92.5/5/2.5) mixture (3 h, 500 rpm). The crude peptides were precipitated from cold diethylether (−20 °C), centrifuged (3 × 5000 rpm, 5 min) washed with cold diethylether, dried under reduced pressure, resolubilized in water, and finally, lyophilized. Then, peptides were dissolved in a solvent A, sonicated, and purified by semi-preparative HPLC equipped with a Nucleosil (Macherey−Nagel) 100-5 C_{18} 250 × 21 mm column using solvent A (95% water, 5% acetonitrile, 0.1% trifluoracetic acid) and solvent B (100% acetonitrile, 0.1% trifluoroacetic acid) with a UV detection at 214 nm. For FSp_3K, the same procedure was applied except solvent A, which is 97% water, 3% acetonitrile, and 0.1% trifluoracetic acid. The resulting solutions were evaporated under reduced pressure and were double-lyophilized. The purity of each peptide was evaluated by analytical reversed-phase HPLC equipped with a Nucleosil (Macherey−Nagel) 100-5 C18 250 × 4.6 mm column using solvent A′ (97% water, 3% acetonitrile, 0.1% formic acid) and solvent B′ (100% acetonitrile, 0.1% formic acid) with a UV detection at 214 nm. Peptides were obtained with 31% (FSp_3E$_2$K), 37% (FSp_3D$_2$K), and 38% (FSp_3K) yield. All chemical characterizations (NMR, HRMS, and HPLC) are provided in the SI.

Antioxidant Activity Assays (General Procedure). HEPES (50 mM, pH 7.4) buffer was treated on a Chelex100 to remove trace metal contaminants from the solution and prevent unwanted reactions before the different tests. The stock solution at 2 mM of iron(III)-nitrate was prepared from an analytical grade reagent in an acidic media (0.1 M HNO_3) to keep iron(III) ion in solution; its exact concentration was checked spectrophotometrically using complexometric titration. The stock solution at 2 mM of calcium(II)-chloride was prepared in H_2O, and the concentration was checked as the same method as in the case of iron(III). Peptides, EDTA, and DFO ligand stock solutions at 2 mM were prepared using HEPES buffer. To perform the tests, a semi-micro quartz cell with a 1 cm optical pathway was used; the sample holder in the spectrophotometer was thermostated at 25 °C by a Peltier temperature controller. For all the experiments, the iron(III)-complexes were prepared 20 min before each antioxidant analysis to assure a complete chelation of the metal ion.

Ascorbate Tests. For a standard assay, a 5 mM ascorbate stock solution was freshly prepared using HEPES buffer at pH 7.4. The absorbance of ascorbate was followed over 10 min at 265 nm (ε = 14,500 M^{-1} cm^{-1}), and at least three independent measurements were carried out. In a total volume of 1 mL, the final concentration of the components was 100 μM with 1:1:1 $AscH^-$:ligand:Fe(III) ratio. In the ascorbate test and in the competition study with Ca(II), the final concentration of the components was also 100 μM with a 1:1:1 (or 2 or 10) $AscH^-$:ligand:Ca(II) ratio or with a 1:1:1:1 (or 10) $AscH^-$:ligand:Fe(III):Ca(II) ratio. The pH was checked at the end of each assay. The reaction was triggered by the addition of ascorbate. As a reference reaction, $AscH^-$ oxidation by ligands alone was also studied. The initial ascorbate oxidation rate was calculated from the slope of $[AscH^-] = f(t)$ (Figure S1).

Amplex Red Assays. The H_2O_2 production was detected by an Amplex Red reagent in the presence of horseradish peroxidase (HRP) forming the compound Resorufin with λ_{abs} = 570 nm. For this assay, all components except the iron(III) ion and Amplex Red reagent were dissolved in 50 mM HEPES buffers. The Amplex Red reagent was dissolved in a DMSO:buffer mixture at a 1:4 ratio. A working solution was first prepared containing 0.8 U/mL HRP and 200 μM Amplex Red reagent in a light-protected tube. A total of 50 μL of this solution was placed in the total volume of 1 mL of reaction mixture. The final concentration of the $AscH^-$ was 200 μM, and the ligand (peptides or DFO):Fe(III):$AscH^-$ ratio was 1:1:4. In the case of EDTA, a ratio of 1:1:20 of EDTA:Fe(III):$AscH^-$ was applied. The $AscH^-$ was the last reagent added, thus initiating the reaction between O_2 and Fe(III); the pH was checked at the end of each reaction. A negative control containing only the working solution in buffer was necessary in order to monitor the background absorbance of the Amplex Red itself. The Resorufin formation was monitored by visible absorption spectroscopy at 570 nm at RT over 45 min. To determine the H_2O_2 concentration, a standard calibration curve was used. To obtain this calibration curve, a 20 mM hydrogen peroxide solution was previously titrated by permanganometry and then diluted successively. The results are summarized in Table S2.

Coumarin-3-carboxylic Acid (3-CCA) Assay. The HEPES buffers disturbed the fluorescence spectra and also had efficient $HO^{\cdot}$ radical scavenging activity, thus pure water treated on Chelex100 was used as solvent and the pH was adjusted by adding 0.1 M NaOH. Thus, all the reagents were dissolved in Milli-Q water except the 3-CCA, since it was only soluble in phosphate buffer (50 mM, pH 7.4). The concentration of the 3-CCA stock solution was 5 mM. In the total volume of 2 mL, the final concentrations of the ascorbate and 3-CCA were both 125 μM, and the ratio of the reaction mixture was ligand (peptides, EDTA or DFO):Fe(III):$AscH^-$ = 1:1:2.5. The pH was checked at the end of the measurement. In the case of EDTA, the amount of all components was 10 times less than that of the other ligand systems (in order to avoid the saturation of the signal due to the high activity of EDTA). For the greater reproducibility of the measured data, each measurement was started by monitoring a blank sample (without any ascorbate) for 5 min, and then the ascorbate was added to the sample. The reaction between 3-CCA and hydroxyl radical generating the fluorescent compound 7-OH-3-CCA was followed over 30 min at 25 °C at λ_{em} = 450 nm (λ_{ex} = 395 nm) by spectrofluorometry. The $HO^{\cdot}$ concentration was determined by a standard calibration curve using commercially available 7-OH-3-CCA.

High Resolution Mass Spectroscopy Studies. For direct injections (HRMS, HRMS/MS, and LC-HRMS experiments), the reaction mixtures were prepared at room temperature in a total volume of 1 mL at pH 7.4 in water (pH was adjusted by 0.1 M NaOH) and analyzed after 24 h. Five different mixtures were studied, including peptide alone, peptide + oxidant (H_2O_2), peptide + Fe(III) + oxidant (H_2O_2), peptide + Fe(III) + oxidant (H_2O_2) + ascorbate, and also, as another control without oxidant, peptide + Fe(III) + ascorbate. Similarly to antioxidant assays, the iron(III)-complexes

https://doi.org/10.1021/acs.inorgchem.1c03085
Inorg. Chem. XXXX, XXX, XXX−XXX

were prepared 20 min before the addition of the redox agent(s) (H_2O_2 and/or ascorbate), to assure a complete chelation of the metal. LC-HRMS experiments were carried out using solvent A (95% water, 5% acetonitrile, 0.1% trifluoracetic acid) and solvent B (100% acetonitrile, 0.1% trifluoroacetic acid) with a 15 min linear gradient (0.5% to 8% solvent B) followed by another 10 min linear gradient (up to 50% B).

Potentiometric Measurements. The pH-potentiometric titrations were investigated in the pH range of 2.0−11.0 at I = 0.1 M $NaNO_3$ ionic force and at T = 298.0 ± 0.1 K. A Dosimat 715 (Metrohm) automatic burette and pH-meter equipped with a semi-micro combined electrode (Metrohm) was used for the titration. The initial concentration of peptides was 1.5×10^{-3} M, using 1:1, 1:2, and 2:1 metal-to-ligand ratios. The titrations were performed with a carbonate free stock solution of sodium hydroxide at known concentration. During the titration, argon was bubbled through the samples to ensure the absence of oxygen and carbon dioxide. The recorded pH readings were converted to hydrogen ion concentration as described by Irving *et al.*[47] Protonation constants of the ligands and the overall stability constants ($\log\beta_{pqr}$) of the complexes were calculated from at least three independent titrations (*ca.* 70 data points per titration) by means of the general computational programs, PSEQUAD[48] and SUPERQUAD using eqs 1 and 2.

$$pM + qH + rL \rightleftharpoons M_pH_qL_r \quad (1)$$

$$\beta_{pqr} = \frac{[M_pL_qH_r]}{[M]^p[L]^q[H]^r} \quad (2)$$

■ ASSOCIATED CONTENT

Supporting Information

The Supporting Information is available free of charge at https://pubs.acs.org/doi/10.1021/acs.inorgchem.1c03085.

Chemical analysis of synthetized peptides, results of antioxidant activity assays, high-resolution mass spectroscopy studies, and complexation studies (PDF)

■ AUTHOR INFORMATION

Corresponding Authors

Katalin Selmeczi − *CNRS, L2CM, Université de Lorraine, F-54000 Nancy, France;* orcid.org/0000-0003-3291-3309; Email: katalin.selmeczi@univ-lorraine.fr

Loic Stefan − *CNRS, LCPM, Université de Lorraine, F-54000 Nancy, France*; Email: loic.stefan@univ-lorraine.fr

Authors

Gizella Csire − *CNRS, LCPM and CNRS, L2CM, Université de Lorraine, F-54000 Nancy, France*

François Dupire − *CNRS, L2CM, Université de Lorraine, F-54000 Nancy, France*

Laetitia Canabady-Rochelle − *CNRS, LRGP, Université de Lorraine, F-54000 Nancy, France;* orcid.org/0000-0003-2772-1556

Complete contact information is available at: https://pubs.acs.org/10.1021/acs.inorgchem.1c03085

Author Contributions

The manuscript was written through contributions of all authors. All authors have given approval to the final version of the manuscript.

Funding

This work was supported by "Impact Biomolecules" project of the "Lorraine Université d'Excellence" (Investissements d'avenir−ANR-15-IDEX-04-LUE).

Notes

The authors declare no competing financial interest.

■ ACKNOWLEDGMENTS

The authors thank P. Lemiere, S. Parant, and M. Achard for technical help. The authors gratefully acknowledge the University of Lorraine, CNRS, and the European Regional Development Funds (Programme opérationnel FEDER-FSE Lorraine et Massif des Vosges 2014-2020, FireLight project: "Photo-bio-active molecules and nanoparticles") for financial support.

■ REFERENCES

(1) Holmström, K. M.; Finkel, T. Cellular Mechanisms and Physiological Consequences of Redox-Dependent Signalling. *Nat. Rev. Mol. Cell Biol.* **2014**, *15*, 411−421.

(2) Schieber, M.; Chandel, N. S. ROS Function in Redox Signaling and Oxidative Stress. *Curr. Biol.* **2014**, *24*, R453−R462.

(3) Pisoschi, A. M.; Pop, A. The Role of Antioxidants in the Chemistry of Oxidative Stress: A Review. *Eur. J. Med. Chem.* **2015**, *97*, 55−74.

(4) Jomova, K.; Valko, M. Advances in Metal-Induced Oxidative Stress and Human Disease. *Toxicology* **2011**, *283*, 65−87.

(5) Liu, Z.; Ren, Z.; Zhang, J.; Chuang, C. C.; Kandaswamy, E.; Zhou, T.; Zuo, L. Role of ROS and Nutritional Antioxidants in Human Diseases. *Front. Physiol.* **2018**, *9*, XXX.

(6) Tian, R.; Xu, J.; Luo, Q.; Hou, C.; Liu, J. Rational Design and Biological Application of Antioxidant Nanozymes. *Front. Chem.* **2021**, *8*, 831.

(7) Kubota, R.; Asayama, S.; Kawakami, H. Catalytic Antioxidants for Therapeutic Medicine. *J. Mater. Chem. B* **2019**, *7*, 3165−3191.

(8) Carocci, A.; Catalano, A.; Sinicropi, M. S.; Genchi, G. Oxidative Stress and Neurodegeneration: The Involvement of Iron. *BioMetals* **2018**, *31*, 715−735.

(9) Poprac, P.; Jomova, K.; Simunkova, M.; Kollar, V.; Rhodes, C. J.; Valko, M. Targeting Free Radicals in Oxidative Stress-Related Human Diseases. *Trends Pharmacol. Sci.* **2017**, *38*, 592−607.

(10) Denoyer, D.; Masaldan, S.; La Fontaine, S.; Cater, M. A. Targeting Copper in Cancer Therapy: "Copper That Cancer". *Metallomics* **2015**, *7*, 1459−1476.

(11) Kasprzak, M. M.; Erxleben, A.; Ochocki, J. Properties and Applications of Flavonoid Metal Complexes. *RSC Adv.* **2015**, *5*, 45853−45877.

(12) Sarmadi, B. H.; Ismail, A. Antioxidative Peptides from Food Proteins: A Review. *Peptides* **2010**, *31*, 1949−1956.

(13) Esfandi, R.; Walters, M. E.; Tsopmo, A. Antioxidant Properties and Potential Mechanisms of Hydrolyzed Proteins and Peptides from Cereals. *Heliyon* **2019**, *5*, No. e01538.

(14) Bechaux, J.; Gatellier, P.; Le Page, J. F.; Drillet, Y.; Sante-Lhoutellier, V. A Comprehensive Review of Bioactive Peptides Obtained from Animal Byproducts and Their Applications. *Food Funct.* **2019**, *10*, 6244−6266.

(15) Lau, J. L.; Dunn, M. K. Therapeutic Peptides: Historical Perspectives, Current Development Trends, and Future Directions. *Bioorganic Med. Chem.* **2018**, *26*, 2700−2707.

(16) Fosgerau, K.; Hoffmann, T. Peptide Therapeutics: Current Status and Future Directions. *Drug Discovery Today* **2015**, *20*, 122−128.

(17) Palomo, J. M. Solid-Phase Peptide Synthesis: An Overview Focused on the Preparation of Biologically Relevant Peptides. *RSC Adv.* **2014**, *4*, 32658−32672.

(18) Kang, N. J.; Jin, H. S.; Lee, S. E.; Kim, H. J.; Koh, H.; Lee, D. W. New Approaches towards the Discovery and Evaluation of Bioactive Peptides from Natural Resources. *Crit. Rev. Environ. Sci. Technol.* **2020**, *50*, 72−103.

(19) Canabady-Rochelle, L. L. S.; Selmeczi, K.; Collin, S.; Pasc, A.; Muhr, L.; Boschi-Muller, S. SPR Screening of Metal Chelating

Peptides in a Hydrolysate for Their Antioxidant Properties. *Food Chem.* **2018**, *239*, 478−485.
(20) Farkas, E.; Sóvágó, I. Metal Complexes of Amino Acids and Peptides. In *Amino Acids, Peptides and Proteins*; The Royal Society of Chemistry: 2017; Vol. *41*, pp. 100−151.
(21) Sóvágó, I.; Várnagy, K.; Lihi, N.; Grenács, Á. Coordinating Properties of Peptides Containing Histidyl Residues. *Coord. Chem. Rev.* **2016**, *327*−*328*, 43−54.
(22) Lv, H.; Shang, P. The Significance, Trafficking and Determination of Labile Iron in Cytosol, Mitochondria and Lysosomes. *Metallomics* **2018**, *10*, 899−916.
(23) Cabantchik, Z. I. Labile Iron in Cells and Body Fluids: Physiology, Pathology, and Pharmacology. *Front. Pharmacol.* **2014**, *5*, 45.
(24) Kurz, T.; Eaton, J. W.; Brunk, U. T. The Role of Lysosomes in Iron Metabolism and Recycling. *Int. J. Biochem. Cell Biol.* **2011**, *43*, 1686−1697.
(25) Csire, G.; Canabady-Rochelle, L.; Averlant-Petit, M. C.; Selmeczi, K.; Stefan, L. Both Metal-Chelating and Free Radical-Scavenging Synthetic Pentapeptides as Efficient Inhibitors of Reactive Oxygen Species Generation. *Metallomics* **2020**, *12*, 1220−1229.
(26) Samaraweera, H.; Zhang, W. G.; Lee, E. J.; Ahn, D. U. Egg Yolk Phosvitin and Functional Phosphopeptides-Review. *J. Food Sci.* **2011**, *76*, R143−R150.
(27) Hegenauer, J.; Saltman, P.; Nace, G. Iron(III)-Phosphoprotein Chelates: Stoichiometric Equilibrium Constant for Interaction of Iron(III) and Phosphorylserine Residues of Phosvitin and Casein. *Biochemistry* **1979**, *18*, 3865−3879.
(28) Khan, I. T.; Nadeem, M.; Imran, M.; Ullah, R.; Ajmal, M.; Jaspal, M. H. Antioxidant Properties of Milk and Dairy Products: A Comprehensive Review of the Current Knowledge. *Lipids Health Dis.* **2019**, *18*, 41.
(29) Kitts, D. D. Antioxidant Properties of Casein-phosphopeptides. *Trends Food Sci. Technol.* **2005**, *16*, 549−554.
(30) Baum, F.; Ebner, J.; Pischetsrieder, M. Identification of Multiphosphorylated Peptides in Milk. *J. Agric. Food Chem.* **2013**, *61*, 9110−9117.
(31) Bernos, E.; Girardet, J. M.; Humbert, G.; Linden, G. Role of the O-Phosphoserine Clusters in the Interaction of the Bovine Milk α_{s1}-, β-, κ-Caseins and the PP3 Component with Immobilized Iron (III) Ions. *Biochim. Biophys. Acta (BBA)- Protein Struct. Mol. Enzymol.* **1997**, *1337*, 149−159.
(32) Mittal, V. A.; Ellis, A.; Ye, A.; Edwards, P. J. B.; Das, S.; Singh, H. Iron Binding to Caseins in the Presence of Orthophosphate. *Food Chem.* **2016**, *190*, 128−134.
(33) Atrián-Blasco, E.; Del Barrio, M.; Faller, P.; Hureau, C. Ascorbate Oxidation by Cu(Amyloid-β) Complexes: Determination of the Intrinsic Rate as a Function of Alterations in the Peptide Sequence Revealing Key Residues for Reactive Oxygen Species Production. *Anal. Chem.* **2018**, *90*, 5909−5915.
(34) Rezende, F.; Brandes, R. P.; Schröder, K. Detection of Hydrogen Peroxide with Fluorescent Dyes. *Antioxid. Redox Signal.* **2018**, *29*, 585−602.
(35) Manevich, Y.; Held, K. D.; Biaglow, J. E. Coumarin-3-Carboxylic Acid as a Detector for Hydroxyl Radicals Generated Chemically and by Gamma Radiation. *Radiat. Res.* **1997**, *148*, 580.
(36) Roginsky, V. A.; Barsukova, T. K.; Bruchelt, G.; Stegmann, H. B. Ion Bound to Ferritin Catalyzes Ascorbate Oxidation: Effects of Chelating Agents. *Biochim. Biophys. Acta (BBA)-Gen. Subj.* **1997**, *1335*, 33−39.
(37) Dean, R. T.; Nicholson, P. The Action of Nine Chelators on Iron-Dependent Radical Damage. *Free Radical Res.* **1994**, *20*, 83−101.
(38) Singh, S.; Hider, R. C. Colorimetric Detection of the Hydroxyl Radical: Comparison of the Hydroxyl-Radical-Generating Ability of Various Iron Complexes. *Anal. Biochem.* **1988**, *171*, 47−54.
(39) Holden, P.; Nair, L. S. Deferoxamine: An Angiogenic and Antioxidant Molecule for Tissue Regeneration. *Tissue Eng. Part B: Rev.* **2019**, *25*, 461−470.
(40) Dalvi, L. T.; Moreira, D. C.; Andrade, R., Jr.; Ginani, J.; Alonso, A.; Hermes-Lima, M. Ellagic Acid Inhibits Iron-Mediated Free Radical Formation. *Spectrochim. Acta, Part A* **2017**, *173*, 910−917.
(41) Ipson, B. R.; Fisher, A. L. Roles of the Tyrosine Isomers Meta-Tyrosine and Ortho-Tyrosine in Oxidative Stress. *Ageing Res. Rev.* **2016**, *27*, 93−107.
(42) Hougland, J. L.; Darling, J.; Flynn, S. Protein Posttranslational Modification. In *Molecular Basis of Oxidative Stress: Chemistry, Mechanisms, and Disease Pathogenesis*; Wiley: 2013, ed. Villamena, F. A., 1st edn, pp. 71−92.
(43) Du, M.; Wu, W.; Ercal, N.; Ma, Y. Simultaneous Determination of 3-Nitro Tyrosine, o-, m-, and p-Tyrosine in Urine Samples by Liquid Chromatography-Ultraviolet Absorbance Detection with Pre-Column Cloud Point Extraction. *J. Chromatogr., B: Anal. Technol. Biomed. Life Sci.* **2004**, *803*, 321−329.
(44) Liu, X. R.; Zhang, M. M.; Zhang, B.; Rempel, D. L.; Gross, M. L. Hydroxyl-Radical Reaction Pathways for the Fast Photochemical Oxidation of Proteins Platform As Revealed by ^{18}O Isotopic Labeling. *Anal. Chem.* **2019**, *91*, 9238−9245.
(45) Luo, M.; Xiao, J.; Sun, S.; Cui, F.; Liu, G.; Li, W.; Li, Y.; Cao, Y. Deciphering Calcium-Binding Behaviors of Casein Phosphopeptides by Experimental Approaches and Molecular Simulation. *Food Funct.* **2020**, *11*, 5284−5292.
(46) Mekmene, O.; Gaucheron, F. Determination of Calcium-Binding Constants of Caseins, Phosphoserine, Citrate and Pyrophosphate: A Modelling Approach Using Free Calcium Measurement. *Food Chem.* **2011**, *127*, 676−682.
(47) Irving, H. M.; Miles, M. G.; Pettit, L. D. A Study of Some Problems in Determining the Stoicheiometric Proton Dissociation Constants of Complexes by Potentiometric Titrations Using a Glass Electrode. *Anal. Chim. Acta* **1967**, *38*, 475−488.
(48) Zekany, L.; Nagypal, I. Psequad. In *Computational Methods for the Determination of Formation Constants*; Leggett, D. J. Ed., Springer: US, 1985; pp. 291−353.

https://doi.org/10.1021/acs.inorgchem.1c03085
Inorg. Chem. XXXX, XXX, XXX−XXX